

## **Measurement of Natural Radioactivity and Assessment of Radiological Hazard Indices of Soil Over the Lithologic Units in Ile-Ife Area, South-West Nigeria**

Authors: Esan, Deborah T, Ajiboye, Yinka, Obed, Rachel I, Ojo, Joshua, Adeola, Mary, et al.

Source: Environmental Health Insights, 16(1)

Published By: SAGE Publishing

URL: <https://doi.org/10.1177/11786302221100041>

---

BioOne Complete ([complete.BioOne.org](https://complete.BioOne.org)) is a full-text database of 200 subscribed and open-access titles in the biological, ecological, and environmental sciences published by nonprofit societies, associations, museums, institutions, and presses.

Your use of this PDF, the BioOne Complete website, and all posted and associated content indicates your acceptance of BioOne's Terms of Use, available at [www.bioone.org/terms-of-use](https://www.bioone.org/terms-of-use).

Usage of BioOne Complete content is strictly limited to personal, educational, and non - commercial use. Commercial inquiries or rights and permissions requests should be directed to the individual publisher as copyright holder.


---

BioOne sees sustainable scholarly publishing as an inherently collaborative enterprise connecting authors, nonprofit publishers, academic institutions, research libraries, and research funders in the common goal of maximizing access to critical research.

# Measurement of Natural Radioactivity and Assessment of Radiological Hazard Indices of Soil Over the Lithologic Units in Ile-Ife Area, South-West Nigeria

Environmental Health Insights  
Volume 16: 1–13  
© The Author(s) 2022  
Article reuse guidelines:  
sagepub.com/journals-permissions  
DOI: 10.1177/11786302221100041



Deborah T Esan<sup>1</sup> , Yinka Ajiboye<sup>1</sup>, Rachel I Obed<sup>2</sup>, Joshua Ojo<sup>3</sup>, Mary Adeola<sup>3</sup> and Mynepalli K Sridhar<sup>2</sup>

<sup>1</sup>Afe Babalola University, Ado-Ekiti, Nigeria. <sup>2</sup>University of Ibadan Faculty of Science, Ibadan, Nigeria. <sup>3</sup>Obafemi Awolowo University, Ife, Nigeria.

**ABSTRACT:** The distribution of natural radioactivity levels of  $^{238}\text{U}$ ,  $^{232}\text{Th}$ , and  $^{40}\text{K}$  in soils overlying the 3 lithologic units within Obafemi Awolowo University, Ile-Ife, Nigeria was investigated to characterize the gamma radiation dose distribution over the lithologies and to assess the radiation hazard due to the natural radionuclides. A thallium-doped cesium iodide detector was employed to determine the activity concentrations of  $^{238}\text{U}$ ,  $^{232}\text{Th}$ , and  $^{40}\text{K}$  in 21 soil samples. The respective average concentrations of the 3 radionuclides are 37.7, 3.2, and 245.6 Bq kg<sup>-1</sup> for granite gneiss, 31.9, 2.8, and 241.1 Bq kg<sup>-1</sup> for banded gneiss, and 21.1, 1.7, and 196.7 Bq kg<sup>-1</sup> for mica schist. The average concentration of  $^{238}\text{U}$  in granite gneiss lithology exceeds the world average value. The evaluated values of radiation hazard parameters including average absorbed dose rate, outdoor annual effective dose and external hazard index are below the recommended limits. The spatial distribution of the radiation hazard parameters evaluated over the lithologies has been delineated. The highest average cancer risk of 1.15 per 10 000 population was obtained for the study area within the soil overlying the banded gneiss lithology. Generally, the radiation hazard from the soils in study area poses no significant health hazard.

**KEYWORDS:** Radioactivity, detector, gamma spectrometry, lithology, natural radionuclide, environmental monitoring

**RECEIVED:** December 21, 2021. **ACCEPTED:** April 14, 2022.

**TYPE:** Ecological Public Health - Original Research Article

**FUNDING:** The author(s) received no financial support for the research, authorship, and/or publication of this article.

**DECLARATION OF CONFLICTING INTERESTS:** The author declared no potential conflicts of interest with respect to the research, authorship, and/or publication of this article.

**CORRESPONDING AUTHOR:** Deborah T Esan, Department of Nursing Science, College of Medicine and Health Sciences, Afe Babalola University, Ado-Ekiti 36000, Nigeria. Emails: esandt@abuad.edu.ng; falodedeborah@gmail.com

## Introduction

Ionizing radiation from natural sources that man is exposed to is an inevitable aspect of life. Human beings everywhere on earth are exposed to ionizing radiation from natural sources.<sup>1</sup> These sources of natural radiation that man is exposed to could either be a cosmic source or primordial source. Cosmic radiations are those which emanate from outer space which release high energy particles into the planet earth.<sup>1</sup> Their interaction with atmospheric particles produces secondary particles that are referred to as cosmogenic radionuclides.<sup>2</sup> The commonest of the radionuclides are the  $^3\text{H}$  and  $^{14}\text{C}$ . Cosmogenic radionuclides contribute about 0.4 mSv of the total annual dose of 2.4 mSv which man is exposed to from natural sources.<sup>3</sup> Of greater significance on the other hand are the primordial sources of radiation that contribute most of man's total radiation from natural sources. The primordial radionuclides are long-lived radionuclides which are present on earth since its formation.<sup>4</sup> The radionuclides are present in the soil, water, building materials, air and also in living organisms.<sup>5-7</sup> The radionuclides are also present in trace levels in the human body.<sup>8,9</sup>

The primordial radionuclides comprise of radionuclides in the  $^{238}\text{U}$  and  $^{232}\text{Th}$  decay series and non-series  $^{40}\text{K}$ . Their half-lives are comparable with the age of the earth contribute the most to the radiation received by humans from natural sources.<sup>3</sup>

\*Mynepalli K Sridhar is now affiliated to University of Ibadan Faculty of Public Health.

The activity concentrations of the primordial radionuclides in the environment play an important role in public health. Soil plays vital role in the transport of primordial radionuclides in the environment. It does not only act as the source, but also serves as a conduit to other environmental media such as air and water.<sup>10</sup> For instance, the atmospheric interface between soil and air enables primordial radionuclide suspension in air.<sup>11,12</sup> In addition, radionuclides can also be leached into both groundwater and surface water.<sup>5</sup> From the perspective of radiation protection, assessment of the level of primordial radionuclides in the environment and the consequent radiation exposure to human is mostly carried out in soil.<sup>13-16</sup> In soil, the distribution of these radionuclides is not uniform.<sup>17,18</sup> On one hand, this is due in part to the transfer of the radionuclides between earth materials such as air to the soil, soil to water, soil to plant, etc.<sup>19,20</sup> On the other hand, the distribution of radionuclides in soils overlying different geologies varies,<sup>21,22</sup> and hence the human exposure due to gamma radiation from the radionuclides in soil also varies from place to place. Soils overlying shales and phosphate rocks in some areas of the world have been reported to exhibit a relatively high level of radioactivity.<sup>3,23</sup> Anthropogenic activities in an area can alter the distribution of the radionuclides in such environment,<sup>24,25</sup> however, the lithological spatial distribution of the radionuclides are useful tools employed in determining gamma radiation distribution and estimation of radiation hazards indices.<sup>10,26,27</sup> The area of study is an academic environment



Creative Commons Non Commercial CC BY-NC: This article is distributed under the terms of the Creative Commons Attribution-NonCommercial 4.0 License (<https://creativecommons.org/licenses/by-nc/4.0/>) which permits non-commercial use, reproduction and distribution of the work without

further permission provided the original work is attributed as specified on the SAGE and Open Access pages (<https://us.sagepub.com/en-us/nam/open-access-at-sage>).  
Downloaded From: <https://complete.bioone.org/journals/Environmental-Health-Insights> on 19 Apr 2024  
Terms of Use: <https://complete.bioone.org/terms-of-use>

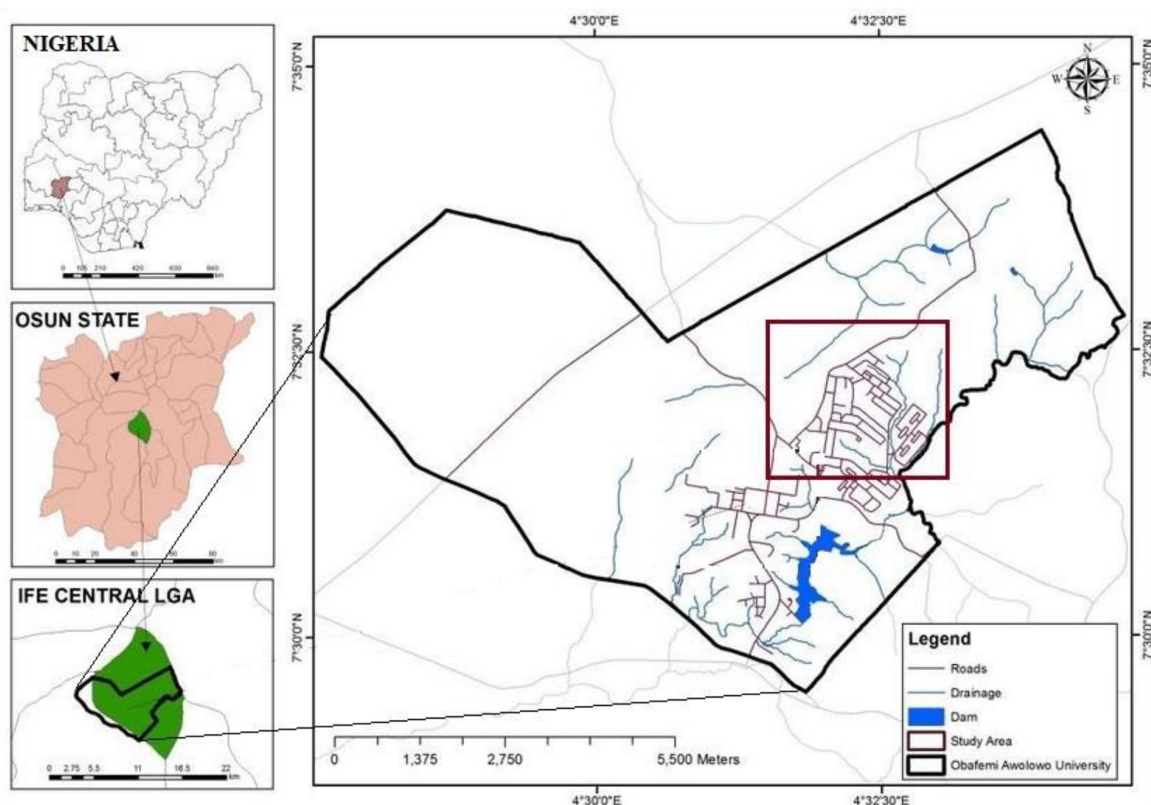


**Figure 1.** Study area map (Inset: maps of Nigeria, Osun State and Ife Central Local Government Area)—Digitized from.<sup>35</sup>

with a population of about 40 000 including staff and students. The buildings in the area are erected over 3 lithologies (banded gneiss, granite gneiss, and mica schist). The inhomogeneity of the geological setting of the area and high soil gas radon concentration ( $>230 \text{ kBq m}^{-3}$ ) has drawn the attention of previous researchers<sup>28,29</sup> to study the distribution of  $^{222}\text{Rn}$  over the lithologies. Often, occurrences of high background radiation have been associated with high radon concentration.<sup>30,31</sup> However, a survey of literature revealed there has been no data regarding the radioactivity of the soil in the area and delineation of the activities across the lithologies.

This study is set out to achieve 2 main objectives. They are (i) to determine the activity concentrations of gamma-emitting radionuclides ( $^{238}\text{U}$ ,  $^{232}\text{Th}$ , and  $^{40}\text{K}$ ) across the different lithologies and (ii) to evaluate the associated radiation hazards. The data and information obtained from this study will serve as a useful tool for planning purposes for limiting the exposure of residents of the area.

## Materials and Method

### *The physical setting of the study area*

The study area is a first-generation University in Nigeria located Ile-Ife town of Osun State. The area lies on the Precambrian basement complex of Southwest Nigeria with geographical coordinates between  $7^{\circ}30''$  and  $7^{\circ}32''$  on the north of the equator and between  $4^{\circ}30''$  and  $4^{\circ}33''$  on the east of the Greenwich meridian (Figure 1). The elevation is between 220 and 380 m above sea level. It lies within the

tropical rain forest region of Nigeria. The area is characterized by 2 distinct seasons—the rainy season usually from April to October, and the dry season from November to March. The annual rainfall ranges between 150 and 3000 mm with varying relative humidity between 40% and 98%.<sup>32</sup> The diurnal temperature varies from  $23^{\circ}\text{C}$  to  $39^{\circ}\text{C}$  with abundant sunshine. The geology of the study area has been extensively studied by Adepelumi et al.<sup>33</sup> The area is underlain with granite gneiss, banded gneiss, and mica schist rock types (Figure 2). The banded gneiss is the oldest recognizable rock. Nearly half of the outcrops in the area are banded gneiss rock types which is the oldest rock and it generally occurs as a low-lying outcrop. It exhibits medium grain and is grayish in color with typical band lines of few millimeters to centimeters in width. There are occurrences of inselbergs forming gentle slope with the surrounding planes which are of granite gneiss rocks with strata of mineral bands. The granite gneiss occupies the north-western part of the study area while the mica schist runs from the northeast through to the south. Banded gneiss is sandwiched between the granite gneiss and mica schist. The landscape is characterized by a steep slope gradient ranging from about 6% to 12%. The bedrock weathered into thick regolith overburden materials that vary from lateritic clay, clayey sand to sand.<sup>34</sup>

### *Samples collection and preparation*

Seven soil samples were spatially collected from each of the 3 lithologies in the study area making a total of 21 soil samples.

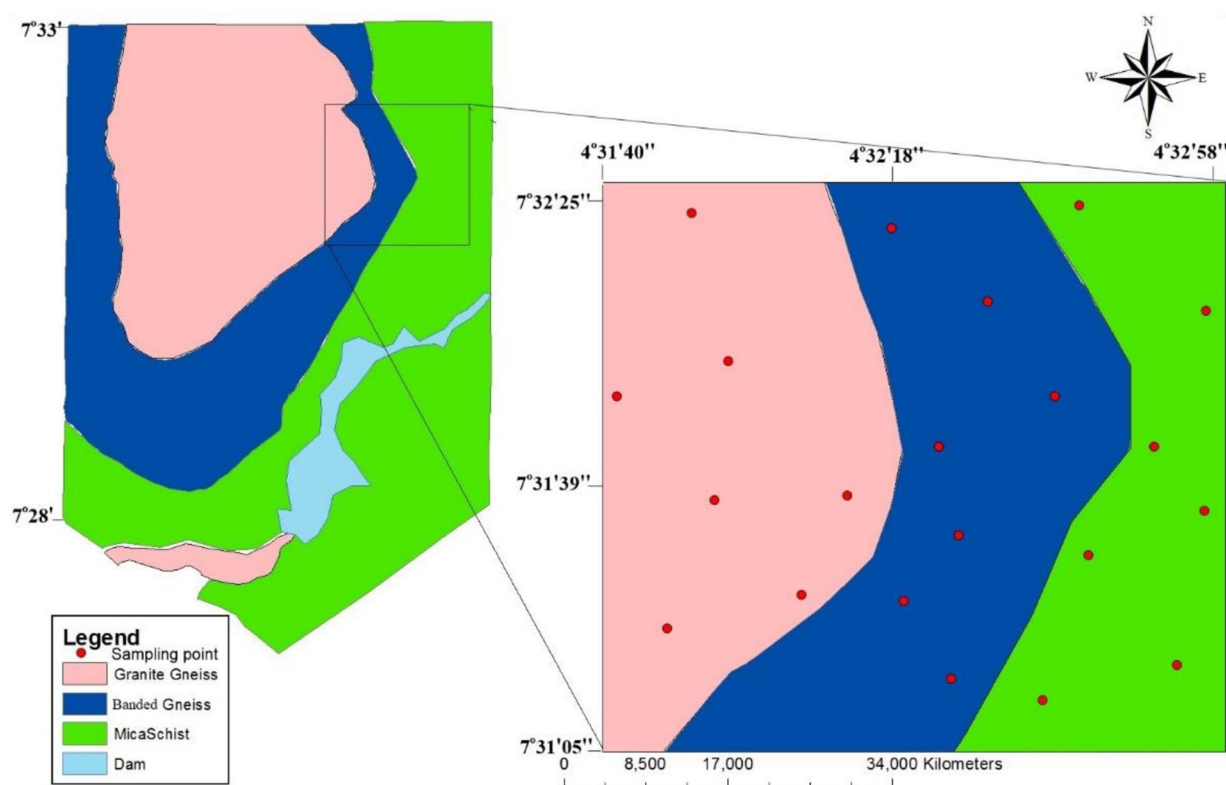


**Figure 2.** Geological map of the study area showing the 3 lithological units and sampling points.

The samples were collected at approximate depths of 15 cm. The sample from each location was collected at the edges of a 1 m<sup>2</sup> land area and also at the center to obtain a representative sample. The samples from all the locations were collected in different polythene bags to avoid sample contamination and labeled appropriately for ease of identification. The samples were thereafter transported to the laboratory for further preparation before spectrometric measurement. At the Laboratory, organic materials were removed from the soil samples and then oven-dried at a temperature of 110°C until a uniform weight was achieved. The dried soil samples were thereafter pulverized and sieved using a 0.2 mm mesh and 200 g of each soil sample was weighted into 7 cm × 9 cm plastic containers. The containers were sealed hermetically with adhesive tapes to prevent the escape of radiogenic gases and then kept for 28 days for the parent radionuclides present in the samples to achieve secular equilibrium with their respective progenies.

#### *Activity concentrations measurement using CsI(Tl) detector*

Spectrometric analysis of the soil samples was carried out using a Thallium-doped Cesium Iodide detector at the Department of Physics and Engineering Physics, Obafemi Awolowo University, Ile-Ife. The spectrometric system comprises of the detector, a URSA II Multichannel Analyser, and a custom-made Pb-shield array. The schematic diagram showing the experimental set-up is shown in Figure 3. A reference

soil standard (IAEA S-375) with known activity from the International Atomic Energy Agency, Vienna, Austria, counted at the same geometry as the samples, was used for the efficiency and energy calibrations of the detector. The efficiency of the detector across the energy spectrum is presented in Figure 4. The IAEA 375 is a homogenized top soil (<20 cm) of 0.3 mm grain size.<sup>30,31</sup> The reference material contains the following radionuclides: <sup>40</sup>K, <sup>90</sup>Sr, <sup>106</sup>Ru, <sup>125</sup>Sb, <sup>129</sup>I, <sup>134</sup>Cs, <sup>137</sup>Cs, <sup>226</sup>Ra, <sup>232</sup>Th, <sup>228</sup>Th, <sup>234</sup>U, <sup>238</sup>U, <sup>238</sup>Pu, <sup>239</sup>+<sup>240</sup>Pu, and <sup>241</sup>Am.<sup>36,37</sup> Typically, spectral resolution of about 7.3% full width at half maximum, FWHM at 662 keV of <sup>137</sup>Cs is specified by detector manufacturers.<sup>38</sup> To minimize statistical uncertainty, the soil samples were counted for 36 000 seconds. The ambient background count was carried out by counting the empty sample container with the same geometry as the sample container used in the actual measurement. The obtained count was subtracted from the sample count to determine the net count due to the radionuclide content of the soil samples. The activity concentrations of <sup>238</sup>U and <sup>232</sup>Th were determined from 352 KeV gamma energy of <sup>214</sup>Pb and 583 KeV gamma energy of <sup>208</sup>Tl respectively since radioactive equilibrium has been achieved between the parent radionuclides and their daughters. The activity of non-series <sup>40</sup>K was determined from the photopeak corresponding to 1460 KeV. The specific activity concentration of each radionuclide in the samples was obtained using the comparative method of analysis. In this method, the activity concentration of the samples is determined by comparing the relevant peak area in the sample



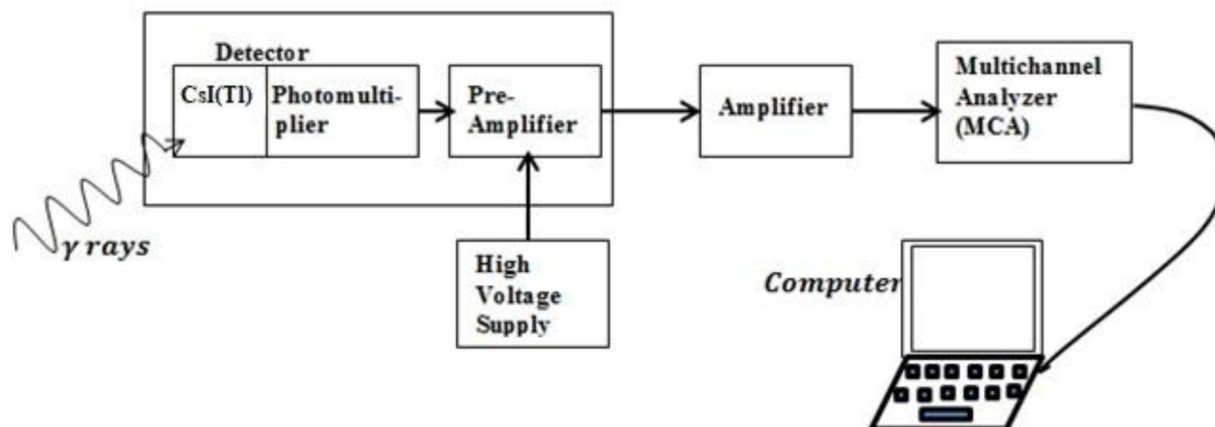


**Figure 3.** Schematic diagram showing the experimental set-up.

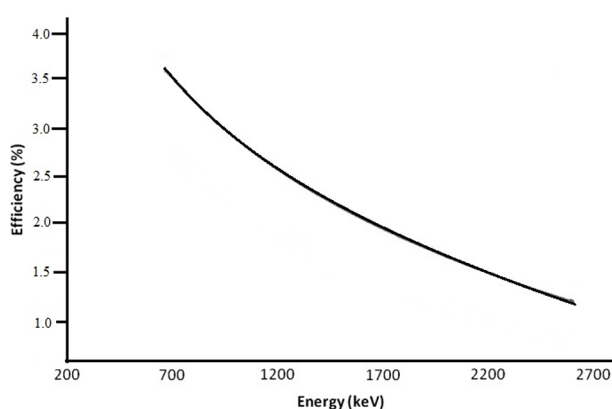


**Figure 4.** Efficiency of the CsI (TI) detector across different energies using the IAEA 375 soil standard.

with area of similar photopeak in a reference standard with already known activity concentration. The activity concentrations of the radionuclides in a sample counted on a detector with a given efficiency for the gamma line of interest were evaluated using equation (1):

$$A(\text{Bq kg}^{-1}) = kn_s \quad (1)$$

where

$$k = (\gamma \cdot \varepsilon \cdot t \cdot M_s)^{-1} \quad (2)$$

where  $n_s$  is the net count rate under the corresponding photopeak,  $\gamma$  is the gamma energy,  $\varepsilon$  is the detector efficiency at that energy,  $t$  is the total counting time (36 000 seconds), and  $M_s$  is the mass of sample in kg. In comparing the unknown activity of the sample  $A_s$  with the known activity of the reference soil standard  $A_{st}$ , equation (3) below was employed.

$$A_s = n \frac{A_{st} \cdot M_{st}}{n_{st} \cdot M_s} \quad (3)$$

Since the counting geometry and detector efficiency, gamma fractional abundance and the counting time are the same for

both the standard and the sample. The subscripts  $st$  and  $s$  represents standard and sample respectively.

The minimum detectable activity concentration of the soil samples which is defined as lower limit of detection (LLD) was estimated using equation (4).<sup>39</sup>

$$LLD = 4.65 \left( \frac{C_{n,b}^{1/2}}{t_b} \right) F \quad (4)$$

where  $C_{n,b}$  is the net background count of a corresponding peak,  $F$  is the conversion factor from counts per second (cps) to  $\text{Bq kg}^{-1}$  and  $t_b$  total time for counting of background radiation in seconds (s). The LLD values of 0.03, 0.01, and 0.10  $\text{Bq kg}^{-1}$  were obtained for  $^{238}\text{U}$ ,  $^{232}\text{Th}$ , and  $^{40}\text{K}$  respectively.

## Evaluation of radiation hazard indices

### Radium equivalent activity

The radium equivalent activity is an index that is used to express the activity due to the radionuclides present in the soil with a single value. Beretka and Mathew,<sup>40,41</sup> suggested the expression to evaluate the radium equivalent activity given in equation (5).

$$Ra_{eq} = A_{Ra} + 1.43A_{Th} + 0.077A_K \quad (5)$$

where  $A_{Ra}$ ,  $A_{Th}$ , and  $A_K$  are the activity concentrations of  $^{226}\text{Ra}$ ,  $^{232}\text{Th}$ , and  $^{40}\text{K}$  respectively. The index is usually estimated based on the assumption that activity values of 370  $\text{Bq kg}^{-1}$  for  $^{226}\text{Ra}$ , 259  $\text{Bq kg}^{-1}$  for  $^{232}\text{Th}$ , and 4810  $\text{Bq kg}^{-1}$  for  $^{40}\text{K}$  all produce the same gamma dose rate.

### Gamma absorbed dose rate

The gamma absorbed dose rate is an index used to quantify the external absorbed gamma dose rate in the air due to the presence of radionuclides in the soil at a height of 1 m above the ground level. It is estimated using the activity concentration

values of  $^{238}\text{U}$ ,  $^{232}\text{Th}$ , and  $^{40}\text{K}$  in equation (6) given by UNSCEAR<sup>3</sup>:

$$D_{\gamma} \left( n\text{Gy } h^{-1} \right) = 0.462 A_U + 0.604 A_{Th} + 0.0417 A_K \quad (6)$$

where  $A_U$ ,  $A_{Th}$ , and  $A_K$  are the activity concentrations of  $^{238}\text{U}$ ,  $^{232}\text{Th}$ , and  $^{40}\text{K}$  respectively.

### Annual effective dose equivalent

The annual outdoor effective dose is estimated from the absorbed gamma dose rate in the air<sup>42-44</sup> using equation (7).

$$D_{eff} \left( m\text{Sv } y^{-1} \right) = D_{\gamma} \left( n\text{Gy } h^{-1} \right) \times 8766 \left( h y^{-1} \right) \times 0.7 \left( \text{Sv Gy}^{-1} \right) \times O.F \quad (7)$$

where 8766 is estimated hours per year, 0.7 is a conversion factor from Gy to Sv and  $O.F$  is the occupancy factor. 0.2 is taken as an occupancy factor outdoor.<sup>3</sup> Equation (7) is compressed as:

$$D_{eff(out)} \left( m\text{Sv } y^{-1} \right) = D_{\gamma} \times 1.23 \times 10^{-3} \quad (8)$$

### External hazard index

The external hazard index is an index which is commonly used to limit absorbed gamma radiation dose to 1.5 mSv  $y^{-1}$ . The index is evaluated using the following relation based on infinitely thick walls without windows and doors<sup>45</sup>:

$$H_{ex} = \frac{A_{Ra}}{370} + \frac{A_{Th}}{259} + \frac{A_K}{4810} \leq 1 \quad (9)$$

$H_{ex}$  values less than unity are considered as not posing significant radiation hazard.

### Excess lifetime cancer risk

The Excess Lifetime Cancer Risk (ELCR) is an index that describes the probability of risk of cancer to the population as a result of exposure from radiation from the soil in an environment.<sup>46</sup> This index is generally used to evaluate the probability of cancer development over a lifetime period, considering 70 years as average life duration for humans at a given exposure level.<sup>46</sup> The ELCR can also be described as a value that represents the number of expected extra cancer cases in a given population that has been exposed to ionizing radiation at a certain dose level. The ELCR is estimated using equation (10):

$$ELCR = D_{eff} \times DL \times RF \quad (10)$$

where  $D_{eff}$  is the annual effective dose equivalent,  $DL$  is the duration of life (70 years), and  $RF$  is the risk factor, 0.05  $\text{Sv}^{-1}$ .<sup>47</sup>

### Statistical analysis

Statistical analysis was performed to separate the means values of  $^{238}\text{U}$ ,  $^{232}\text{Th}$ , and  $^{40}\text{K}$  in soil overlying the 3 lithologies. The data were subjected to Analysis of Variance (ANOVA) and the means were separated using Tukey test. All analyses were carried out using Minitab, version 17.0 and Excel softwares.

### Results

The activity concentrations of  $^{238}\text{U}$ ,  $^{232}\text{Th}$ , and  $^{40}\text{K}$  in soil overlying the 3 lithologies in the study area: granite gneiss, banded gneiss, and mica schist with their radium equivalent activities are presented in Table 1. As presented in the table, the activity concentrations of  $^{238}\text{U}$  in granite gneiss, banded gneiss, and mica schist range from  $34.1 \pm 3.5$  to  $43.1 \pm 4.5$  Bq  $\text{kg}^{-1}$ ,  $25.8 \pm 2.7$  to  $43.9 \pm 4.5$  Bq  $\text{kg}^{-1}$ , and  $12.2 \pm 1.3$  to  $26.5 \pm 2.7$  Bq  $\text{kg}^{-1}$  respectively. Their respective mean values are  $37.7 \pm 2.9$ ,  $31.9 \pm 6.3$ , and  $21.2 \pm 4.1$  Bq  $\text{kg}^{-1}$  respectively. The overall average activity concentration of  $^{238}\text{U}$  is  $30.3 \pm 8.2$  Bq  $\text{kg}^{-1}$ . The values of activity concentrations for  $^{232}\text{Th}$  in soil samples range from  $3.0 \pm 0.5$  to  $3.7 \pm 0.6$  Bq  $\text{kg}^{-1}$ ,  $2.2 \pm 0.4$  to  $3.6 \pm 0.6$  Bq  $\text{kg}^{-1}$ , and  $0.9 \pm 0.2$  to  $2.2 \pm 0.4$  Bq  $\text{kg}^{-1}$  for granite gneiss, banded gneiss, and mica schist respectively. Their average values are  $3.2 \pm 0.2$ ,  $2.8 \pm 0.4$ , and  $1.7 \pm 0.4$  Bq  $\text{kg}^{-1}$  respectively, while the overall average activity concentration of  $^{232}\text{Th}$  is  $2.6 \pm 0.7$  Bq  $\text{kg}^{-1}$ . The activity concentrations of  $^{40}\text{K}$  range from  $209.7 \pm 7.0$  to  $318.8 \pm 10.6$  Bq  $\text{kg}^{-1}$ ,  $220.6 \pm 7.4$  to  $265.2 \pm 8.9$  Bq  $\text{kg}^{-1}$ , and  $114.3 \pm 3.8$  to  $272.9 \pm 9.1$  Bq  $\text{kg}^{-1}$  for granite gneiss, banded gneiss, and mica schist range respectively. Their respective average activities are  $245.6 \pm 35.2$ ,  $242.1 \pm 12.9$ , and  $196.7 \pm 44.4$  Bq  $\text{kg}^{-1}$  respectively with the overall average activity of  $228.1 \pm 40.3$  Bq  $\text{kg}^{-1}$ . The mean values of the concentrations of  $^{238}\text{U}$ ,  $^{232}\text{Th}$ , and  $^{40}\text{K}$  in soil overlying the 3 lithologies were significantly different ( $P < .05$ ), but the mean values obtained under Granite Gneiss and Banded Gneiss were similar ( $P > .05$ ). The differences in the means occurred in soil overlying Mica Schist for  $^{232}\text{Th}$ , and  $^{40}\text{K}$ , but were all similar for  $^{40}\text{K}$ . The world average values of the activity concentrations of the radionuclides ( $^{40}\text{K}$ ,  $^{238}\text{U}$ ,  $^{232}\text{Th}$ ) in the soil of the study area are presented in Table 1. The spatial distribution of the activities of  $^{40}\text{K}$ ,  $^{238}\text{U}$ ,  $^{232}\text{Th}$ , and the radium equivalent activity in the study area is presented in Figures 5 to 8. The Pearson's correlation coefficient obtained for the 3 radionuclide pairs are .60, .62 and .98 for  $^{40}\text{K}/^{238}\text{U}$ ,  $^{40}\text{K}/^{232}\text{Th}$ , and  $^{238}\text{U}/^{232}\text{Th}$  respectively.

The radium equivalent activities for the soil samples obtained from the 3 lithologies were evaluated based on the activities of  $^{238}\text{U}$ ,  $^{232}\text{Th}$ , and  $^{40}\text{K}$  using equation (1). The radium equivalent activities of the soil samples overlying the granite gneiss, banded gneiss, and mica schist lithologies range from 55.4 to 69.3 Bq  $\text{kg}^{-1}$ , 47.3 to 67.3 Bq  $\text{kg}^{-1}$ , and 22.3 to 46.3 Bq  $\text{kg}^{-1}$  with average values of  $61.2 \pm 4.8$ ,  $54.5 \pm 7.1$ , and

**Table 1.** Activity concentrations of radionuclides and their radium equivalent activities in the granite gneiss (GG), banded gneiss (BG), and mica schist (MS) lithologies.

SAMPLE ID	$^{40}\text{K}$ (BQ KG $^{-1}$ )	$^{238}\text{U}$ (BQ KG $^{-1}$ )	$^{232}\text{Th}$ (BQ KG $^{-1}$ )	RAEQ (BQ KG $^{-1}$ )
GG1	318.8 $\pm$ 10.6	37.3 $\pm$ 3.9	3.2 $\pm$ 0.6	66.4
GG2	271.1 $\pm$ 9.1	43.1 $\pm$ 4.5	3.7 $\pm$ 0.6	69.3
GG3	242.7 $\pm$ 8.1	39.9 $\pm$ 4.1	3.1 $\pm$ 0.5	63.0
GG4	233.2 $\pm$ 7.8	34.6 $\pm$ 3.6	3.0 $\pm$ 0.5	56.9
GG5	226.4 $\pm$ 7.6	37.1 $\pm$ 3.8	3.0 $\pm$ 0.5	58.9
GG6	209.8 $\pm$ 7.0	37.6 $\pm$ 3.9	3.3 $\pm$ 0.6	58.4
GG7	216.9 $\pm$ 7.2	34.1 $\pm$ 3.5	3.2 $\pm$ 0.5	55.4
Mean (GG)	245.6a $\pm$ 35.2	37.7a $\pm$ 2.9	3.2a $\pm$ 0.2	61.2a $\pm$ 4.8
BG1	265.2 $\pm$ 8.9	37.2 $\pm$ 3.8	3.1 $\pm$ 0.5	62.0
BG2	246.7 $\pm$ 8.2	26.4 $\pm$ 2.7	2.4 $\pm$ 0.4	48.8
BG3	237.0 $\pm$ 7.9	43.9 $\pm$ 4.5	3.6 $\pm$ 0.6	67.3
BG4	239.8 $\pm$ 8.0	25.8 $\pm$ 2.7	2.2 $\pm$ 0.4	47.3
BG5	235.0 $\pm$ 7.9	26.3 $\pm$ 2.7	2.4 $\pm$ 0.4	47.8
BG6	220.6 $\pm$ 7.37	33.4 $\pm$ 3.5	2.8 $\pm$ 0.5	54.4
BG7	250.7 $\pm$ 8.37	30.4 $\pm$ 3.1	2.8 $\pm$ 0.5	53.7
Mean (BG)	242.1a $\pm$ 12.9	31.9a $\pm$ 6.3	2.8a $\pm$ 0.4	54.5a $\pm$ 7.1
MS1	223.6 $\pm$ 7.5	22.9 $\pm$ 2.4	1.9 $\pm$ 0.3	42.8
MS2	180.8 $\pm$ 6.0	26.5 $\pm$ 2.7	2.2 $\pm$ 0.4	43.5
MS3	188.5 $\pm$ 6.3	22.8 $\pm$ 2.4	1.8 $\pm$ 0.3	39.9
MS4	189.8 $\pm$ 6.3	20.7 $\pm$ 2.1	1.7 $\pm$ 0.3	37.7
MS5	206.7 $\pm$ 6.9	21.0 $\pm$ 2.2	1.7 $\pm$ 0.3	39.2
MS6	114.3 $\pm$ 3.8	12.2 $\pm$ 1.3	0.9 $\pm$ 0.2	22.3
MS7	272.9 $\pm$ 9.1	22.7 $\pm$ 2.3	1.8 $\pm$ 0.3	46.3
Mean (MS)	196.7a $\pm$ 44.4	21.2b $\pm$ 4.1	1.7b $\pm$ 0.4	38.8b $\pm$ 7.3
Overall mean	228.1 $\pm$ 40.3	30.3 $\pm$ 8.2	2.6 $\pm$ 0.7	51.5 1 $\pm$ 1.4
World average	420	33	45	-

Means that do not share a letter are significantly different.

38.8  $\pm$  7.3 Bq kg $^{-1}$  respectively. Table 2 presents a comparative study of the activity concentrations of  $^{238}\text{U}$ ,  $^{232}\text{Th}$ , and  $^{40}\text{K}$  obtained in this study with previous studies by other researchers in Nigeria.

The radiation hazard indices for granite gneiss, banded gneiss, and mica schist were evaluated and presented in Table 3. The absorbed gamma dose rate for granite gneiss lithology varies from 26.7 to 33.5 nGy h $^{-1}$  with an average value of 29.6 nGy

h $^{-1}$ . For banded gneiss, the value ranges from 23.2 to 30.1 nGy h $^{-1}$  with an average value of 26.5 nGy h $^{-1}$ . Also, the value ranges from 10.9 to 23.0 nGy h $^{-1}$  with an average value of 19.0 nGy h $^{-1}$  for mica schist. Their means were significantly different at 5% level of significance, with both Granite and Banded Gneisses giving similar ( $P > .05$ ) absorbed dose, annual effective dose, external hard index, and excess lifetime cancer risk. However, their values were significantly lower with Mica Schist

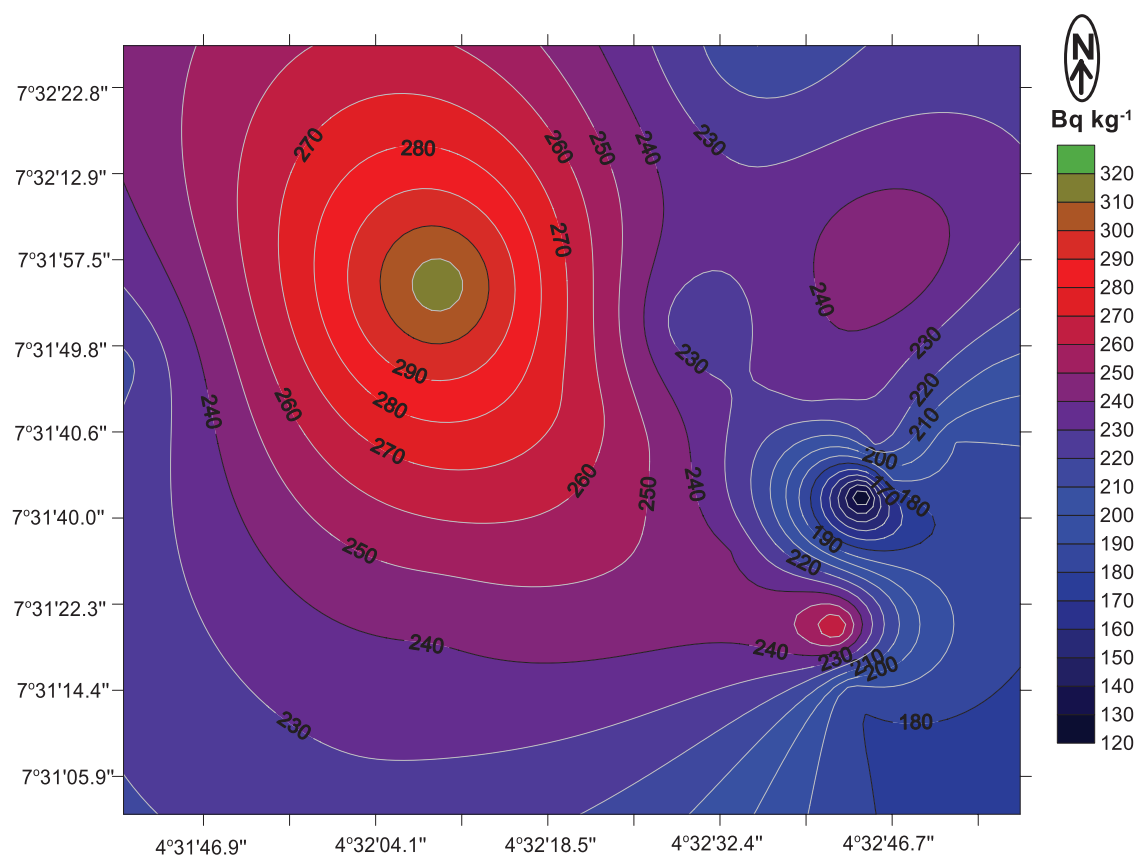


Figure 5. Spatial distribution of  $^{40}\text{K}$  within the study area.

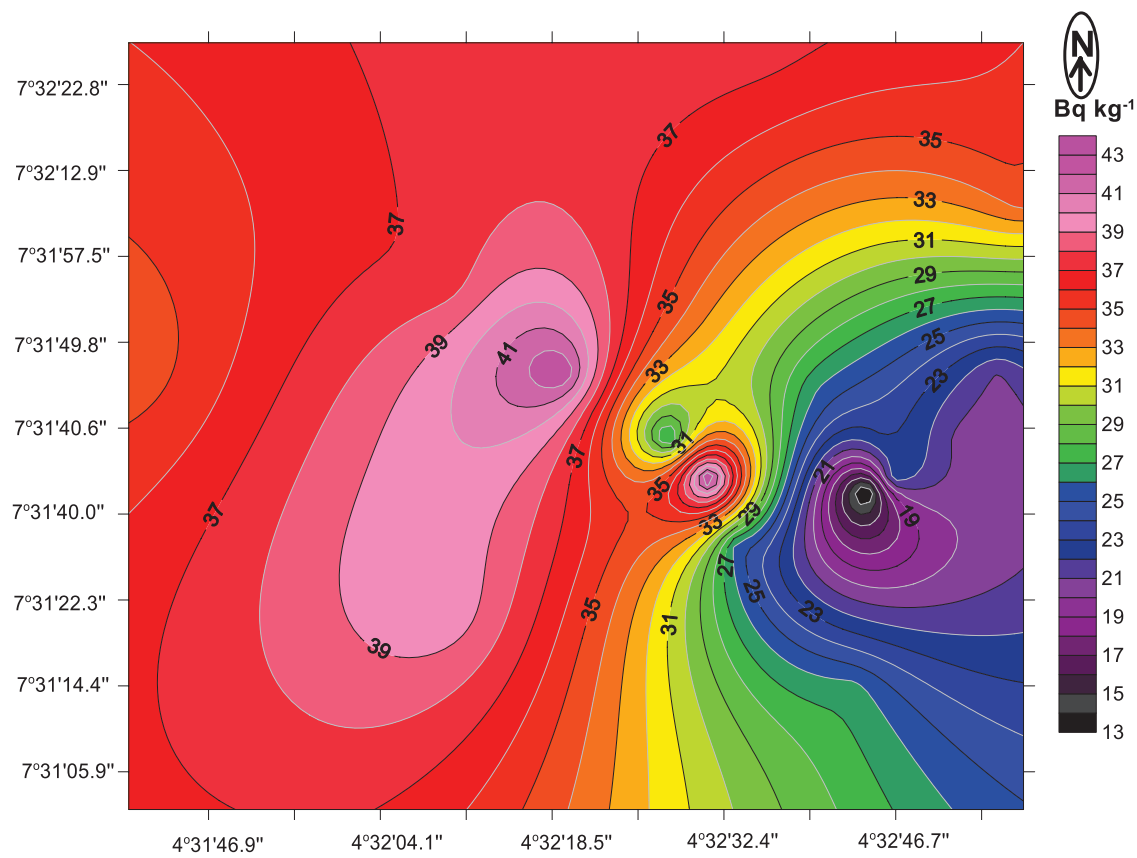
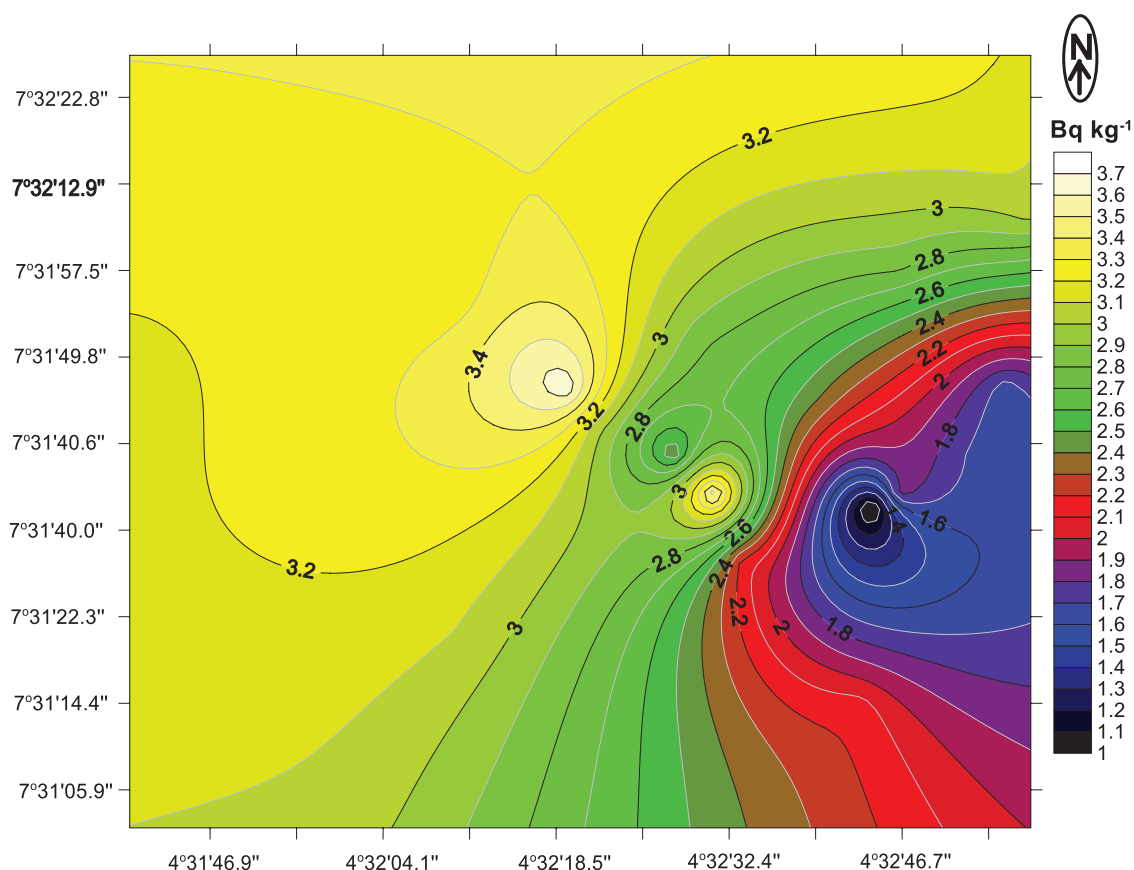
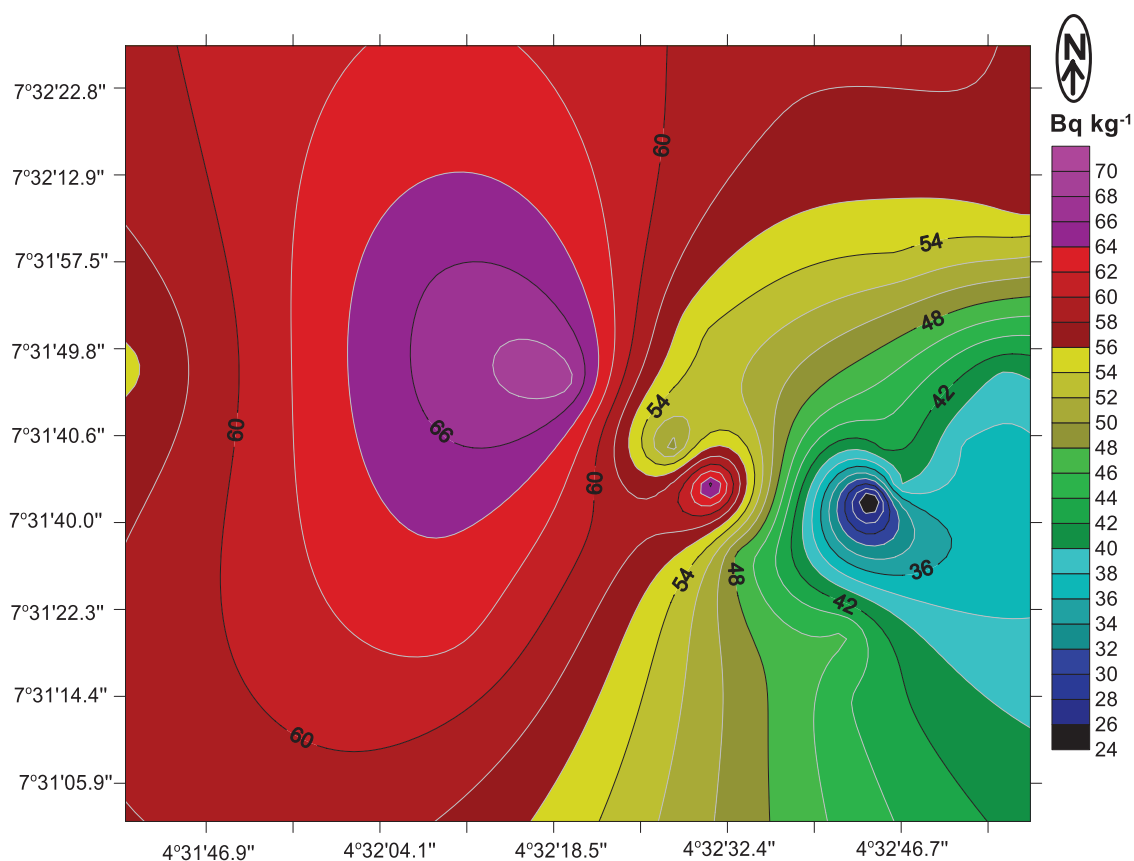


Figure 6. Spatial distribution of  $^{238}\text{U}$  within the study area.





**Figure 7.** Spatial distribution of  $^{232}\text{Th}$  within the study area.



**Figure 8.** Spatial distribution of radium equivalent activity within the study area.

**Table 2.** Comparison of activity concentrations of  $^{238}\text{U}$ ,  $^{232}\text{Th}$ , and  $^{40}\text{K}$  in present study with similar studies in Nigeria.

REGION	$^{238}\text{U}$ (BQ KG <sup>-1</sup> )	$^{232}\text{Th}$ (BQ KG <sup>-1</sup> )	$^{40}\text{K}$ (BQ KG <sup>-1</sup> )	REFERENCE
Owo, Ondo State	64.6	110.2	1190.1	Aladeniyi et al <sup>48</sup>
Orlu, Imo State	4.2	1.6	134.1	Mbonu and Ben <sup>49</sup>
Igbokoda, Ondo State	11.5	9.9	194.7	Ajanaku et al <sup>50</sup>
Ado-Odo, Ogun State	40.4	94.4	134.2	Joel et al <sup>51</sup>
Esan Land, Edo State	2.1	6.9	57.8	Popoola et al <sup>52</sup>
Benue State	22.5	8.9	164.6	Kungur et al <sup>53</sup>
Nigeria (All 6 geopolitical zones of Nigeria)	33.9	12.4	73.3	Farai et al <sup>54</sup>
Ile-Ife, Osun State	30.3	2.6	228.1	Present Study

**Table 3.** Radiation doses and health hazard index in granite gneiss (GG), banded gneiss (BG), and mica schist (MS) lithologies.

SAMPLE ID	ABSORBED DOSE (NGY H <sup>-1</sup> )	ANNUAL EFFECTIVE DOSE (MSV Y <sup>-1</sup> ) OUTDOOR	EXTERNAL HAZARD INDEX (H <sub>EX</sub> )	EXCESS LIFETIME CANCER RISK (10 <sup>-3</sup> )
GG1	32.5	0.04	0.18	0.140
GG2	33.5	0.04	0.19	0.140
GG3	30.4	0.04	0.17	0.140
GG4	27.6	0.03	0.15	0.105
GG5	28.4	0.03	0.16	0.105
GG6	28.1	0.03	0.16	0.105
GG7	26.7	0.03	0.15	0.105
Mean (GG)	29.59a	0.04a	0.17a	0.120a
BG1	30.1	0.04	0.17	0.140
BG2	23.9	0.03	0.13	0.105
BG3	32.3	0.04	0.18	0.140
BG4	23.2	0.03	0.13	0.105
BG5	23.4	0.03	0.13	0.105
BG6	26.3	0.03	0.15	0.105
BG7	26.2	0.03	0.15	0.105
Mean (BG)	26.50a	0.03a	0.15a	0.115a
MS1	21.0	0.03	0.12	0.105
MS2	21.1	0.03	0.12	0.105
MS3	19.5	0.02	0.11	0.070
MS4	18.5	0.02	0.10	0.070
MS5	19.3	0.02	0.11	0.070
MS6	10.9	0.01	0.06	0.035
MS7	23.0	0.03	0.13	0.105
Mean (MS)	19.04b	0.02b	0.10b	0.080b
Overall mean	25.0 ± 5.4	0.03 ± 0.01	0.14 ± 0.03	0.11 ± 0.03

Means that do not share a letter are significantly different.

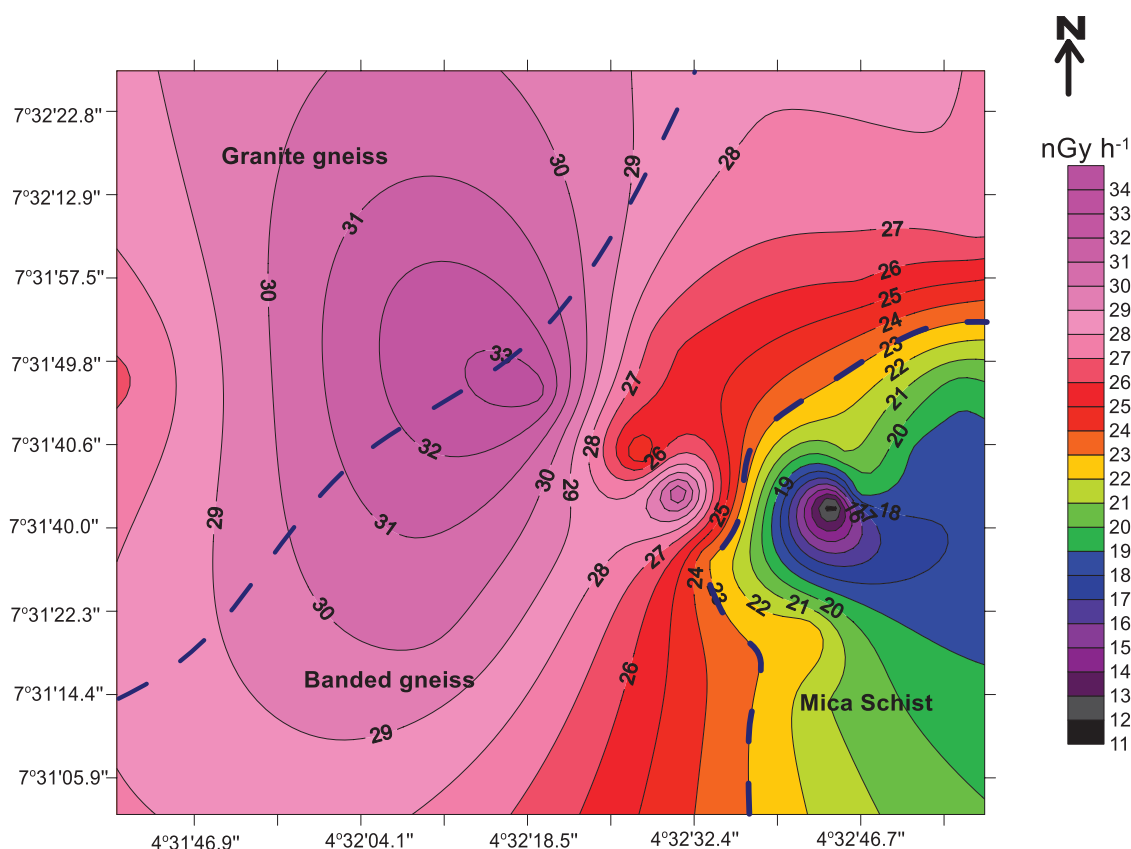


**Figure 9.** Interpolated estimation map of the absorbed gamma dose rate.

( $P < .05$ ), when compared to those observed at Granite Gneiss and Banded Gneiss. A contour map showing the spatial distribution of the absorbed gamma dose rate in the study area is presented in Figure 9.

The average outdoor annual effective dose due to gamma radiation from the radionuclides in the soil is estimated to be 0.04, 0.03, and 0.02 mSv y<sup>-1</sup> for granite gneiss, banded gneiss, and mica schist respectively. Also, the evaluated external hazard index for granite gneiss, banded gneiss, and mica schist are 0.17, 0.15, and 0.10 respectively.

The evaluated excess lifetime cancer risk for granite gneiss, banded gneiss, and mica schist are  $0.120 \times 10^{-3}$ ,  $0.115 \times 10^{-3}$ , and  $0.080 \times 10^{-3}$  respectively. These values correspond respectively to the probabilities 1.2, 1.15, and 0.8 persons in a population of 10 000 developing cancer with 70 years considered as average lifetime duration.

## Discussion

The average value of activity concentration of  $^{238}\text{U}$  obtained for soil samples collected from the granite gneiss lithologies exceeds the world average value of  $33 \text{ Bq kg}^{-1}$ ,<sup>3</sup> whereas, that of banded gneiss and mica schist are below. This is attributable to high uranium mineralization of granitic rocks.<sup>55</sup> Generally, the average activity concentrations for  $^{238}\text{U}$ ,  $^{232}\text{Th}$ , and  $^{40}\text{K}$  across all the lithologies are below their respective world average values. The activity concentration of  $^{232}\text{Th}$  across the area is

generally much lower to the world average value with the ratio of about (1:17). The results of the activity concentration of radionuclides in the 3 lithologies exhibit low values of standard deviation indicating that each of the radionuclides is uniformly distributed across each of the lithologies. Also, the spatial spread of the radionuclides across the 3 lithologies as presented in Figures 5 to 7 shows minimum variability. The spatial gradient of  $^{40}\text{K}$  (Figure 5) clearly delineates 2 regions of concentrations:  $180 \leq K \leq 230 \text{ Bq kg}^{-1}$  which falls mostly on the south east of the study area dominated by mica schist and  $230 \leq K \leq 300 \text{ Bq kg}^{-1}$  in the north west area dominated by granite gneiss. Similarly, the spatial gradient of  $^{238}\text{U}$  (Figure 6) shows that mica schist region exhibits lowest range of concentrations, typically between  $15 \text{ Bq kg}^{-1}$  and  $31 \text{ Bq kg}^{-1}$ . The granite gneiss and banded gneiss regions have concentration distributions between  $31 \text{ Bq kg}^{-1}$  and  $41 \text{ Bq kg}^{-1}$ . The spatial distribution of  $^{232}\text{Th}$  (Figure 7) shows spatial concentration gradient with the granite gneiss, banded gneiss and mica schist lithologies exhibiting highest, medium and lowest concentrations respectively.

Comparison of the level of radionuclide concentrations obtained in this study with similar studies previously carried out in Nigeria by other researchers is shown in Table 2. The study revealed that average  $^{238}\text{U}$  concentration in this study is higher than those obtained in parts of Imo, Ondo, Edo, and Benue<sup>48-54</sup> States. The value however compares with the

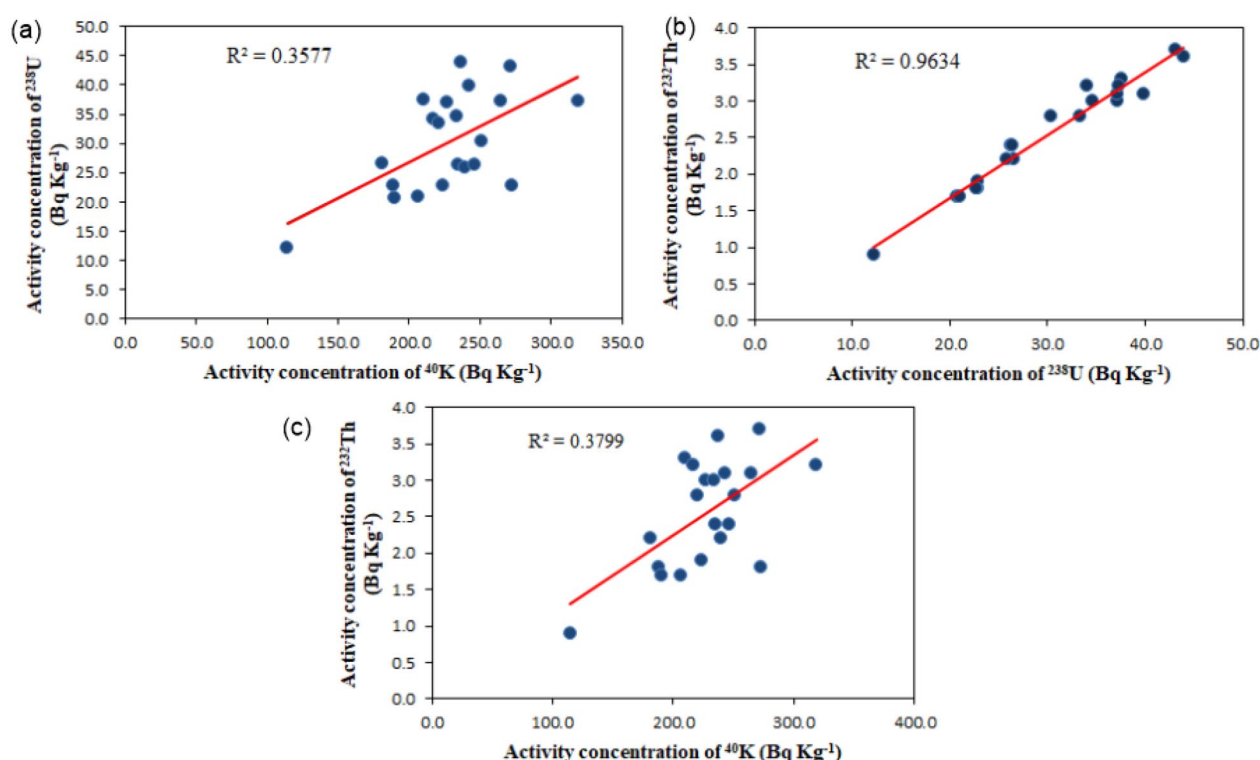


**Figure 10.** Correlation plots of (a)  $^{238}\text{U}$  against  $^{40}\text{K}$ , (b)  $^{232}\text{Th}$  against  $^{238}\text{U}$ , and (c)  $^{232}\text{Th}$  against  $^{40}\text{K}$ .

average value obtained for the 6 geopolitical zones of Nigeria.<sup>54</sup> The average concentration of  $^{232}\text{Th}$  obtained in this study is lower than those obtained in other parts of the country except for Imo State.<sup>48–54</sup> However,  $^{40}\text{K}$  average concentration in the present study is higher than those obtained in most part of the country except for Ondo State.

Test of correlation between the 3 radionuclide pairs:  $^{40}\text{K}/^{238}\text{U}$ ,  $^{40}\text{K}/^{232}\text{Th}$ , and  $^{238}\text{U}/^{232}\text{Th}$  as presented in Figure 10 revealed a strong positive correlation which is significant at .01 level (2-tailed). This also indicates uniform distribution of the radionuclides in the soils of the study area.

The granite gneiss lithology exhibits the highest radium equivalent activity. The average radium equivalent activity for the 3 lithologies is such that  $\text{Ra}_{\text{eq}}(\text{granite gneiss}) > \text{Ra}_{\text{eq}}(\text{banded gneiss}) > \text{Ra}_{\text{eq}}(\text{mica schist})$ . The  $\text{Ra}_{\text{eq}}$  values for the 3 lithologies are much less than the recommended limit of  $370 \text{ Bq kg}^{-1}$  for building materials. The implication is that the soil in all the lithologies is suitable for use in building materials. Comparison of interpolated map for  $^{238}\text{U}$  in Figure 6 with the interpolated map of radium equivalent activity in Figure 8 shows that  $^{238}\text{U}$  is the major contributor to the radium equivalent activity across the area as the contour lines in both maps exhibit similar trend.

The average outdoor annual effective dose due to gamma radiation from the radionuclides in the soil is estimated to be 0.04, 0.03, and  $0.02 \text{ mSv y}^{-1}$  for granite gneiss, banded gneiss, and mica schist respectively. These values are much less than the recommended limit of  $1 \text{ mSv y}^{-1}$ .<sup>42</sup> Also, the evaluated external hazard index for granite gneiss, banded gneiss, and mica schist are 0.17, 0.15, and 0.10 respectively. These values

are much less compared to the maximum permissible level of 1. This implies that exposure to gamma radiation from the soil is of insignificant consequence to health. The gamma radiation absorbed dose rate within the geologic areas is of the order:  $\gamma_{\text{granite gneiss}} > \gamma_{\text{banded gneiss}} > \gamma_{\text{mica schist}}$ . The delineated gamma radiation dose rate of the area shows that granite gneiss lithology has dose rates between the range of 29 and  $33 \text{ nGy h}^{-1}$ , banded gneiss lithology has between 23 and  $32 \text{ nGy h}^{-1}$  and mica schist lithology has between 11 and  $23 \text{ nGy h}^{-1}$ . The gamma dose rate values obtained for all the soil samples in all the lithologies are below the world average value of  $60 \text{ nGy h}^{-1}$ .<sup>3</sup>

The evaluated excess lifetime cancer risk for granite gneiss, banded gneiss, and mica schist are  $0.120 \times 10^{-3}$ ,  $0.115 \times 10^{-3}$ , and  $0.080 \times 10^{-3}$  respectively. These values correspond respectively to the probabilities 1.2, 1.15, and 0.8 persons in a population of 10000 developing cancer with 70 years considered as average lifetime duration. These values are less than the average value of  $0.2 \times 10^{-3}$ <sup>56</sup> and  $0.4 \times 10^{-3}$ <sup>57</sup> obtained in similar studies within Ekiti State—a basement complex region in Southwest Nigeria and across 6 Southwest States of Nigeria respectively.

## Conclusion

A pilot study to evaluate the distribution of  $^{238}\text{U}$ ,  $^{232}\text{Th}$ , and  $^{40}\text{K}$  in soil across 3 geological formations within Obafemi Awolowo University, Ile-Ife, Nigeria has been carried out. The average activity concentrations of  $^{238}\text{U}$ ,  $^{232}\text{Th}$ , and  $^{40}\text{K}$  in all the lithologies were found to be below the world average value except for

that of  $^{238}\text{U}$  in the granite gneiss lithology. The obtained values for the radiation hazard indices were also found to be below the recommended limits. The study showed that lithologies on which soils are overlying is a strong contributing factor to the concentrations of  $^{238}\text{U}$ ,  $^{232}\text{Th}$ , and  $^{40}\text{K}$  found in them. Also, the absorbed dose rate, annual effective dose, external hard index, and excess lifetime cancer risk were also found to vary across the lithologies. This study, however, provides information on the distribution of external gamma radiation from the soil in the study area. It can be concluded on the basis of the evaluated radiation hazard indices that the soil in the study area do not pose significant health hazard to the members of the public.

## Acknowledgements

The authors wish to appreciate the Management of Afe Babalola University for releasing the researcher to conduct the fieldwork.

## Author contribution

Conceptualization: DTE, RIO and MKS; Methodology: DTE, JO, MA, YA; Formal analysis and investigation: DTE, YA, MA and JO; Writing - original draft preparation: DTE and YA; Writing - review and editing: DTE, YA and JO; Funding acquisition: Not Applicable; Resources: DTE; Supervision: MKS and RIO.

## Ethics Approval

Ethical clearance was obtained from UI/UCH ethics review committee of the University of Ibadan, Ibadan (Protocol number: UI/EC/16/0352).

## ORCID iD

Deborah T Esan  <https://orcid.org/0000-0002-3896-8207>

## REFERENCES

- Susam LA, Alan HY, Yilmaz A, et al. Cosmic radiation exposure calculations for international and domestic flights departs from Istanbul and Ankara. *Radiat Prot Dosimetry*. 2020;192:61-68.
- Mekhaldi F, Adolphi F, Herbst K, Muscheler R. The signal of solar storms embedded in cosmogenic radionuclides: detectability and uncertainties. *J Geophys Res Space Phys*. 2021;126:e2021JA029351.
- UNSCEAR. Sources and effects of ionizing radiation. ANNEX B: Exposures from natural radiation sources. UNSCEAR Report; 2000:97-99.
- Al-Khawlani A, Khan A, Pathan J. Review on studies in natural background radiation. *Radiat Prot Environ*. 2018;41:215.
- Arunima S, Lekshmi R, Jojo PJ, Mayeen Uddin K. A study on leaching of primordial radionuclides  $^{232}\text{Th}$  and  $^{40}\text{K}$  to water bodies. *Radiat Phys Chem*. 2021;188:109658.
- Sarker MS, Rahman R, Siraz MM, Khandaker MU, Yeasmin S. The presence of primordial radionuclides in powdered milk and estimation of the concomitant ingestion dose. *Radiat Phys Chem*. 2021;188:109597.
- Fakhri Y, Sarafraz M, Pilevar Z, et al. The concentration and health risk assessment of radionuclides in the muscle of tuna fish: a worldwide systematic review and meta-analysis. *Chemosphere*. 2022;289:133149.
- Almayahi BA, Tajuddin AA, Jaafar MS. Measurements of natural radionuclides in human teeth and animal bones as markers of radiation exposure from soil in the Northern Malaysian Peninsula. *Radiat Phys Chem*. 2014;97:56-67.
- Muikku M, Li W. Natural radionuclides in human hair. In: Preddy VR, ed. *Handbook of Hair in Health and Disease*. Wageningen Academic Publishers; 2012:316-330.
- Ribeiro FC, Silva JI, Lima ES, do Amaral Sobrinho NM, Perez DV, Lauria DC. Natural radioactivity in soils of the state of Rio de Janeiro (Brazil): radiological characterization and relationships to geological formation, soil types and soil properties. *J Environ Radioact*. 2018;182:34-43.
- Sýkora I, Povinec PP. Natural and anthropogenic radionuclides on aerosols in Bratislava air. *J Radioanal Nucl Chem*. 2020;325:245-252.
- Whicker JJ, Breshears DD, McNaughton M, Chastenot de Gery MJ, Bullock C. Radionuclide resuspension across ecosystems and environmental disturbances. *J Environ Radioact*. 2021;233:106586.
- Abbasi A, Kurnaz A, Turhan Ş, Mirekhtiary F. Radiation hazards and natural radioactivity levels in surface soil samples from dwelling areas of North Cyprus. *J Radioanal Nucl Chem*. 2020;324:203-210.
- Garba NN, Ramli AT, Saleh MA, Gabdo HT. Natural radioactivity and associated radiation hazards in soil of Kelantan, Malaysia. *Hum Ecol Risk Assess*. 2019;25:1707-1717.
- Alajeeeli A, Elmahroug Y, Mohammed S, Trabelsi A. Determination of natural radioactivity and radiological hazards in soil samples: Alhadba and Abuscab agricultural projects in Libya. *Environ Earth Sci*. 2019;78:1-8.
- Jananee B, Rajalakshmi A, Thangam V, Bharath KM, Sathish V. Natural radioactivity in soils of Elephant hills, Tamilnadu, India. *J Radioanal Nucl Chem*. 2021;329:1261-1268.
- Bala P, Mehra R, Ramola RC. Distribution of natural radioactivity in soil samples and radiological hazards in building material of Una, Himachal Pradesh. *J Geochem Explor*. 2014;142:11-15.
- Cowart JB, Burnett WC. The distribution of uranium and thorium decay-series radionuclides in the environment—a review. *J Environ Qual*. 1994;23:651-662.
- Alharbi A, El-Taher A. A study on transfer factors of radionuclides from soil to plant. *Life Science Journal*. 2013;10:532-539.
- Twining JR, Payne TE, Itakura T. Soil-water distribution coefficients and plant transfer factors for  $^{134}\text{Cs}$ ,  $^{85}\text{Sr}$  and  $^{65}\text{Zn}$  under field conditions in tropical Australia. *J Environ Radioact*. 2004;71:71-87.
- Dragović S, Janković-Mandić L, Dragović R, Đorđević M, Đokić M, Kovačević J. Lithogenic radionuclides in surface soils of Serbia: spatial distribution and relation to geological formations. *J Geochem Explor*. 2014;142:4-10.
- Patra AC, Sahoo SK, Tripathi RM, Puranik VD. Distribution of radionuclides in surface soils, Singhbhum Shear Zone, India and associated dose. *Environ Monit Assess*. 2013;185:7833-7843.
- Sahin L, Hafizoglu N, Çetinkaya H, Manisa K, Bozkurt E, Biçer A. Assessment of radiological hazard parameters due to natural radioactivity in soils from granite-rich regions in Kütahya Province, Turkey. *Isotopes Environ Health Stud*. 2017;53:212-221.
- Atipo M, Olarinoye O, Awojoyogbe B. Comparative analysis of NORM concentration in mineral soils and tailings from a tin-mine in Nigeria. *Environ Earth Sci*. 2020;79:1-17.
- Ram R, Kalnins C, Pownceby MI, et al. Selective radionuclide co-sorption onto natural minerals in environmental and anthropogenic conditions. *J Hazard Mater*. 2021;409:124989.
- Gulan L, Valjarevic A, Milenkovic B, Stevanovic V, Milic G, Stajic JM. Environmental radioactivity with respect to geology of some Serbian spas. *J Radioanal Nucl Chem*. 2018;317:571-578.
- Alomari AH, Saleh MA, Hashim S, Alsayaheem A, Abukashabeh A. Statistical relationship between activity concentrations of radionuclides  $^{226}\text{Ra}$ ,  $^{232}\text{Th}$ ,  $^{40}\text{K}$ , and  $^{137}\text{Cs}$  and geological formations in surface soil of Jordan. *Isotopes Environ Health Stud*. 2019;55:211-226.
- Ajayi T, Adepelumi A. Reconnaissance soil-gas radon survey over the faulted crystalline area of Ile-Ife, Nigeria. *Environ Geol*. 2002;41:608-613.
- Esan DT, Sridhar MKC, Obed R, et al. Determination of residential soil gas radon risk indices over the lithological units of a Southwestern Nigeria University. *Sci Rep*. 2020;10:7368.
- Nalukudiparambil J, Gopinath G, Ramakrishnan RT, Surendran AK. Groundwater radon ( $^{222}\text{Rn}$ ) assessment of a coastal city in the high background radiation area (HBRA), India. *Arab J Geosci*. 2021;14:1-7.
- Nugraha ED, Hosoda M, Kusdiana K, et al. Comprehensive exposure assessments from the viewpoint of health in a unique high natural background radiation area, Mamuju, Indonesia. *Sci Rep*. 2021;11:14578.
- Akinbode OM, Eludoyin AO, Fashae OA. Temperature and relative humidity distributions in a medium-size administrative town in southwest Nigeria. *J Environ Manag*. 2008;87:95-105.
- Adepelumi A, Ako B, Ajayi T. Groundwater contamination in the basement-complex area of Ile-Ife, southwestern Nigeria: a case study using the electrical-resistivity geophysical method. *Hydrogeol J*. 2001;9:611-622.
- Adepelumi AA, Ajayi TR, Ako BD, Ojo AO. Radon soil-gas as a geological mapping tool: case study from basement complex of Nigeria. *Environ Geol*. 2005;48:762-770.
- Popoola O, Salami A, Adepoju K, Alaga A, Oloko-Oba M, Badru R. Updating Landuse Map of Obafemi Awolowo University campus using low-cost unmanned aerial vehicle (UAV) image. *J Geogr Environ Earth Sci Int*. 2016;8:1-7.
- IAEA. International Atomic Energy Agency Reference sheet – reference material IAEA-375. 2000. Accessed February 3, 2022. <https://nucleus.iaea.org/sites/ReferenceMaterials/Pages/IAEA-375.aspx>



37. Altitzoglou T, Bohnstedt A. Characterisation of the IAEA-375 soil reference material for radioactivity. *Appl Radiat Isot.* 2016;109:118-121.
38. Martin PG, Hutson C, Payne L, et al. Validation of a novel radiation mapping platform for the reduction of operator-induced shielding effects. *J Radiol Prot.* 2018;38:1097-1110.
39. Gbadamosi MR, Afolabi TA, Banjoko OO, et al. Spatial distribution and lifetime cancer risk due to naturally occurring radionuclides in soils around tar-sand deposit area of Ogun State, southwest Nigeria. *Chemosphere.* 2018;193:1036-1048.
40. Beretka J, Matthew PJ. Natural radioactivity of Australian building materials, industrial wastes and by-products. *Health Phys.* 1985;48:87-95.
41. Zhou Z, Yang Z, Sun Z, Liao Q, Guo Y, Chen J. Multidimensional pollution and potential ecological and health risk assessments of radionuclides and metals in the surface soils of a uranium mine in East China. *J Soils Sediments.* 2020;20:775-791.
42. Almayahi BA, Tajuddin AA, Jaafar MS. Radiation hazard indices of soil and water samples in Northern Malaysian Peninsula. *Appl Radiat Isot.* 2012;70:2652-2660.
43. Jibiri NN, Isinkaye MO, Momoh HA. Assessment of radiation exposure levels at Alaba e-waste dumpsite in comparison with municipal waste dumpsites in southwest Nigeria. *J Radiat Res Appl Sci.* 2014;7:536-541.
44. Saini K, Bajwa BS. Mapping natural radioactivity of soil samples in different regions of Punjab, India. *Appl Radiat Isot.* 2017;127:73-81.
45. Krieger R. Radioactivity of construction materials. *Betonwerk Fertigteil Technik.* 1981;47:468-473.
46. Taskin H, Karavus M, Ay P, Topuzoglu A, Hidioglu S, Karahan G. Radionuclide concentrations in soil and lifetime cancer risk due to gamma radioactivity in Kırklareli, Turkey. *J Environ Radioact.* 2009;100:49-53.
47. International Commission on Radiological Protection. 1990 Recommendations of the International Commission on Radiological Protection. ICRP Publication 60. Ann. ICRP 21 (1-3). Elsevier Health Sciences; 1990.
48. Aladeniyi K, Olowookere C, Oladele BB. Measurement of natural radioactivity and radiological hazard evaluation in the soil samples collected from Owo, Ondo State, Nigeria. *J Radiat Res Appl Sci.* 2019;12:200-209.
49. Mbonu CC, Ben UC. Assessment of radiation hazard indices due to natural radioactivity in soil samples from Orlu, Imo State, Nigeria. *Heliyon.* 2021;7:e07812.
50. Ajanaku O, Ilori AO, Ibitola GA, Faturoti OB. Assessment of natural radioactivity and associated dose rates in surface soils around Oluwa Glass Industry Environments, Igbokoda, Ondo State, Southwestern Nigeria. *Phys Sci Int J.* 2018;20:1-13.
51. Joel ES, Maxwell O, Adewoyin OO, et al. Investigation of natural environmental radioactivity concentration in soil of coastal area of Ado-Odo/Ota Nigeria and its radiological implications. *Sci Rep.* 2019;9:4219.
52. Popoola FA, Fakeye OD, Basiru QB, Adesina DA, Sulola MA. Assessment of radionuclide concentration in surface soil and human health risk associated with exposure in two higher institutions of Esan land, Edo State, Nigeria. *J Appl Sci Environ Manag.* 2020;23:22679-32284.
53. Kungur ST, Ige TA, Ikoy BA. Analysis of natural radionuclides and evaluation of radiation hazard indices in soil samples from Benue state, Nigeria. *Int J Innov Res Sci Eng.* 2020;5:1765-1769.
54. Farai IP, Obed RI, Jibiri NN. Soil radioactivity and incidence of cancer in Nigeria. *J Environ Radioact.* 2006;90:29-36.
55. Sarangi AK, Singh AS. Vein type uranium mineralisation in Jaduguda, uranium deposits, Singhbhum, India. In *Proceedings of the International Symposium on understanding the Genesis of Ore Deposits to Meet the Demands of 21st Century, Association on the Genesis of Ore Deposits*, Moscow held on 15 May 2006.
56. Isinkaye MO, Ajiboye Y. Natural radioactivity in surface soil of urban settlements in Ekiti State, Nigeria: baseline mapping and the estimation of radiological risks. *Arab J Geosci.* 2022;15:1-16.
57. Ibikunle SB, Arogunjo AM, Ajayi OS. Characterization of radiation dose and excess lifetime cancer risk. *J Forensic Sci Crim Inves.* 2018;10:555793.